

Chemical and Photometric Evolution of the Local Group Galaxy NGC 6822 in a Cosmological Context

Leticia Carigi

Instituto de Astronomía, UNAM, Apdo. Postal 70-264, México 04510 D.F., Mexico
carigi@astroscu.unam.mx

Pedro Colín

Centro de Radioastronomía y Astrofísica, UNAM, Apdo. Postal 72-3, 58089 Morelia, Michoacán, Mexico
p.colin@astrosmo.unam.mx

and

Manuel Peimbert

Instituto de Astronomía, UNAM, Apdo. Postal 70-264, México 04510 D.F., Mexico
peimbert@astroscu.unam.mx

ABSTRACT

Based on the photometric properties of NGC 6822 we derive a robust star formation history. Adopting this history we compute 15 models of galactic chemical evolution. All of them match present-day photometric properties. The dark halo mass in all models evolves according to the mass assembly history predicted by a Λ CDM cosmology. We model the evolution of the baryonic mass aggregation history in this cosmological context assuming that part of the gas available for accretion never falls into the system due to two different physical processes. For seven models we assume that during accretion the universal baryon fraction is reduced by reionization only. The best model of this first group, a complex model with an early outflow, fits the observed gaseous mass, and the O/H, C/O, and Fe/O present-day values. This model requires a lower upper mass limit for the IMF than that of the solar vicinity, in agreement with recent results by other authors. We have also computed eight models where, in addition to reionization, the accreted baryon fraction is reduced by large-scale shock heating. The best model of this series, that also requires an early outflow and a lower upper mass limit for the IMF, can marginally fit the gaseous mass and the O/H and C/O observed values.

Subject headings: galaxies: abundances—galaxies: evolution—galaxies: individual NGC 6822—galaxies: irregular—Local Group

1. Introduction

The main aim of this paper is to produce chemical evolution models of the irregular galaxy NGC 6822. These models will be used to look for consistency with the cosmological context of galaxy formation as well as to study the possible presence of outflows from this object to the intergalactic

medium.

In the field of chemical evolution often it is argued that a model for a given galaxy is far from being unique. In this paper we use as many observational constraints as possible to try to obtain a robust model with the idea of getting closer to a unique solution. The constraints used include: gas mass, chemical abundances, integrated colors,

and a star formation history derived from observations. On the other hand the models used a gas infall history derived from the hierarchical standard Λ CDM cosmology. The models also used the IMF and the yields that reproduce the chemical evolution of the solar neighborhood and the Galactic disk (Carigi et al. 2005).

NGC 6822 is particularly suited for chemical evolution models because its star formation history is well known (Wyder 2001, 2003), its present chemical composition might permit to decide if outflows to the intergalactic medium have been produced by this galaxy. NGC 6822, unlike the Magellanic Clouds, has not lost a significant amount of mass due to tidal effects.

NGC 6822 is a member of the local group that apparently has not been affected by tidal effects from the Milky Way or M31 (Sawa & Fujimoto 2005). There has been no recent interaction between NGC 6822 and these two galaxies because: i) NGC 6822 is located 495 kpc away from our Galaxy and is receding from it at a radial velocity of 44 km s^{-1} (e.g. Trimble 2000), and ii) NGC 6822 is also located at 880 kpc from M31, it is separated from M31 by more than 90 degrees in the sky, and M31 is approaching our Galaxy at 121 km s^{-1} (Trimble 2000).

An open problem in the study of the chemical evolution of irregular galaxies is the cause of the difference between the observed effective oxygen yield and the oxygen yield predicted by closed box chemical evolution models. One solution to this problem might be due to the presence of O-rich galactic outflows (e.g. Garnett 2002). Several lines of reasoning indicate that O-rich outflows produced by gas rich irregular galaxies are unlikely. Carigi et al. (1995, 1999), based on the C/O and O/H values for nearby irregular galaxies, have found that O-rich outflows have not played an important role in their evolution. A similar result has been obtained by Larsen et al. (2001), based on the N/O versus O/H relationship. These results indicate that O-rich outflows do not play a major role in the evolution of irregular galaxies. Another solution to the O yield problem might be due to the presence of dark matter (e.g. Carigi et al. 1999).

The importance of outflows to the intergalactic medium from nearby irregular galaxies depends on many factors, like their total mass, the distri-

bution in time and space of their star formation, and the presence of tidal effects (e.g. Legrand et al. 2001; Tenorio-Tagle et al. 2003; Martin 2003; Fragile et al. 2004; Fujita et al. 2004, and references therein).

In most galaxy chemical evolution models the infall of gas of primordial composition is modeled assuming a parametric form (e.g., Lanfranchi & Matteucci 2003). Here we will take a cosmological approach: the rate at which gas is accreted by the galaxy will depend on how the mass, dark and baryonic, falls into the galaxy (the mass assembly history, MAH), and the reionization history of the universe. The MAH in turn depends on the assumed cosmology and the total mass of the galaxy (e.g., Avila-Reese et al. 1998; van den Bosch 2002). For a halo of a given mass, there is an ensemble of possible MAHs. In this paper we will take the mean MAH (defined in section 3.3) as representative of the MAH of NGC 6822. Before the epoch of reionization, the history of the infalling gas is simply related by a constant to the MAH, afterwards the amount of gas accreted by the galaxy will depend on how fast the mass of the dark halo and the filtering mass grow with time (Gnedin 2000; Kravtsov, Gnedin, & Klypin 2004). We will assume also that the gas infalling history is not altered by processes such as ram pressure or tidal striping. These assumptions are supported by the absence of warm-hot gas associated to the Local Group and by the fact that this galaxy is isolated.

In section 2 we define different masses present in an irregular galaxy and their role in chemical evolution models. The total mass and the halo mass assembly history within a Λ CDM cosmology are derived in sections 3.1 – 3.3. In section 3.4 we discuss two scenarios for the baryonic mass building of the galaxy, one in which the reionization of the universe reduces the galaxy baryon fraction, below the universal one; and another in which in addition to reionization the galaxy baryon fraction is also reduced by large-scale shock heating. In section 4 we estimate the gaseous mass and discuss the present day chemical composition to be fitted by the models. In section 5 we determine the variation of the star formation rate and the luminosity with time. In section 6 we discuss the evidence in favor of gas outflows. In section 7 we present the general characteristics of the chemical evolution

models. In section 7.1 we discuss the large infall models, hereinafter L models, where the effect of gas shock heating is not considered. In section 7.2 we discuss the small infall models, hereinafter S models, where the effect of gas shock heating is considered, this effect prevents a substantial fraction of baryons from reaching the galaxy. In sections 8 and 9 we present the discussion and the conclusions.

2. Definitions

We can define the total mass, M_{total} , as

$$M_{total} = M_{bar} + M_{DM}, \quad (1)$$

where M_{bar} is the baryonic mass, and M_{DM} is the non-baryonic mass.

M_{bar} can be expressed as

$$M_{bar} = M_{sub} + M_{stars} + M_{rem} + M_{gas}, \quad (2)$$

where M_{sub} is the mass in substellar objects (with stellar mass, m , lower than $0.1 M_{\odot}$), and has also been called the baryonic dark matter, M_{stars} is the mass of objects with $m > 0.1 M_{\odot}$, and M_{rem} is the mass in compact stellar remnants.

M_{gas} can be approximated by

$$M_{gas} = M(\text{H I}) + M(\text{He I}) + M(\text{H}_2), \quad (3)$$

where we have neglected the ionized and the heavy element components. M_{gas} is also given by

$$M_{gas} = M_{bar}(\text{accreted}) - M_{gas}(\text{outflow}) - (M_{sub} + M_{stars} + M_{rem}) + M_R, \quad (4)$$

where $M_{bar}(\text{accreted})$ is the baryonic mass accreted from the intergalactic medium during the galaxy formation, $M_{gas}(\text{outflow})$ is the baryonic mass ejected to the intergalactic medium during the galactic evolution, and M_R is the mass returned to the ISM by the evolution of the stars.

We define the ratio of the baryonic mass accreted by the galaxy to the total mass as

$$f_{acc} = M_{bar}(\text{accreted})/M_{total}, \quad (5)$$

and the ratio of the baryonic mass that remains in the galaxy to the total mass as

$$f_{gal} = f_{acc} - M_{gas}(\text{outflow})/M_{total}. \quad (6)$$

In this paper, galaxy and halo are synonymous.

3. Total Mass: M_{total}

3.1. M_{total} from direct observations of the rotation curve

A high-resolution rotation curve that extends to 5 kpc has been determined for this galaxy by Wel-drake et al. (2003) using the Australian Telescope Compact Array. Inside this radius, R , the mass of the galaxy given by $M_{lower} = \frac{V_c^2 R}{G}$ is $3.5 \times 10^9 M_{\odot}$, where we are assuming that the circular velocity, V_c , is equal to the *rotational* velocity determined observationally from the gaseous component of the disk and amounts to 55 km s^{-1} . With an observed baryonic mass of $4.3 \times 10^8 M_{\odot}$ (see sections 4 and 7) we find that NGC 6822 is a galaxy dominated by dark matter with $M_{bar}/M_{lower} = 0.12$, inside $R < 5 \text{ kpc}$.

3.2. M_{total} from the cosmological context

The total mass of a galaxy is a model dependent quantity. Here we will use a cosmologically motivated model to estimate the mass of the galaxy in question. Cosmological collisionless N-body simulations show that density profiles of dark matter (DM) halos can be described well by the NFW profile (Navarro, Frenk, & White 1995, 1996, 1997)

$$\rho_{\text{NFW}}(r) = \frac{\rho_0}{r/r_s(1+r/r_s)^2}. \quad (7)$$

The characteristic radius r_s is the radius where the logarithmic derivative of ρ_{NFW} is -2 , while the characteristic density ρ_0 is given by $\rho_0 = 4\rho_{\text{NFW}}(r_s)$. The NFW profile can also be characterized by a concentration parameter, $c_{vir} \equiv R_{vir}/r_s$, and by the virial circular velocity $V_{vir} = \sqrt{GM_{total}/R_{vir}}$, where M_{total} is the virial mass of the galaxy. The virial radius, R_{vir} , can be defined as the radius where the average halo density is δ times the mean density of the universe according to the spherical top-hat model. Here δ is a number that depends on epoch and cosmological parameters ($\Omega_0, \Omega_{\Lambda}$); for a flat (0.3,0.7) Λ CDM

model $\delta \sim 334$ at the present epoch. In practice, we use cosmology to infer a relationship between the maximum circular velocity, V_{peak} , and V_{vir} , that is given by

$$V_{vir}^2 = 4.63 \frac{f(c_{vir})}{c_{vir}} V_{peak}^2 \quad (8)$$

(Bullock et al. 2001), where $f(c_{vir}) = \ln(1 + c_{vir}) - c_{vir}/(1 + c_{vir})$. We thus can estimate the total mass of the halo once V_{peak} and c_{vir} are given.

We use as V_{peak} the rotational velocity at the outermost measured point. The mass of the halo may be underestimated because: i) the rotation curve for this galaxy may still rise beyond this radius and ii) we are neglecting any contribution from the gas velocity dispersion. The concentration of a DM halo depends on many parameters such as nature of the dark matter, halo mass, epoch, normalization of the power spectrum, etc. Here we will assume the ‘‘concordance’’ Λ CDM model ($\Omega_0 = 0.3$, $\Omega_\Lambda = 0.7$, $h = 0.7$, $\sigma_8 = 0.9$) where h is the Hubble constant in units of $100 \text{ km s}^{-1} \text{ Mpc}^{-1}$ and σ_8 is the rms of the mass fluctuations computed with the top-hat window of radius $8 h^{-1} \text{ Mpc}$. If we take the median concentration estimated using the model by Bullock et al. (2001) and $V_{peak} = 55 \text{ km s}^{-1}$ from Weldrake et al. (2003) we find $M_{total} = 2.6 \times 10^{10} M_\odot$. This is the total mass that we will assign to NGC 6822 that implies an $R_{vir} = 76.3 \text{ kpc}$ and $M_{lower}/M_{total} = 0.13$.

The adopted M_{total} implies that baryons at present contribute to the galaxy mass budget with only 1.65%, such small values seem to be typical of dwarf galaxies.

3.3. Mass assembly history: MAH

Within the CDM galaxy formation paradigm a halo grows in a hierarchical fashion: self-bound structures form from bottom to top through the accretion and merging of smaller structures. A halo of a given mass today can arise from one of many possible mass aggregation histories. We use the recipe described in appendix A of van den Bosch (2002), which is based on the extended Press-Schechter formalism (Bond et al. 1991; Bower 1991; Lacey & Cole 1993), to derive the mean MAH for our given particular cosmological model and halo mass.

van den Bosch (2002) finds, after experimenting with a variety of fitting functions, that the MAHs are well fitted by the following parametric form:

$$\log \left[\frac{M(z)}{M_0} \right] = -0.301 \left[\frac{\log(1+z)}{\log(1+z_f)} \right]^\nu, \quad (9)$$

where $M(z)$ and M_0 are the mass of the halo at z and $z = 0$, respectively, and z_f and ν are free parameters. According to this expression, z_f is defined as the redshift where half of the mass of the halo is acquired, and it is 1.50 for the total mass and cosmological context assumed in this paper. Based on Figure 6 of van den Bosch we took two additional models with extreme values of z_f , given by $\log(1+z_f) = 0.4 \pm 0.1$, to cover the scatter in the mass assembly histories. The mean MAH is computed assuming $z_f = 1.50$, the slow and fast MAHs are those computed adopting $z_f = 1.00$ and $z_f = 2.16$, respectively. Figure 1 shows the MAHs of these models (solid for mean and dotted lines for slow and fast).

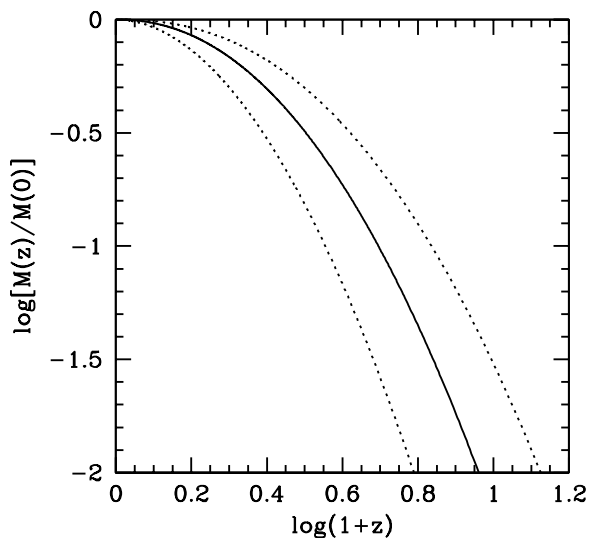


Fig. 1.— The mean mass assembly history in units of the present-day mass (solid line) computed using the recipe described in appendix A of van den Bosch (2002) with $z_f = 1.50$ (the redshift where the halo acquires half of its mass). The scatter in the diagram has been incorporated by using two extreme values for z_f namely 1.00 and 2.16 (dotted lines).

3.4. M_{gas} versus time

A high fraction of baryons $\sim 90\%$ in the present-day universe do not reside in galaxies, the missing baryons (Fukugita & Peebles 2004). They can be in virialized regions of halos (hot gas in hydrostatic equilibrium), in a diffuse phase with overdensities $\delta < 1000$ ($\delta \equiv \rho/\bar{\rho} - 1$, where $\bar{\rho}$ is the mean density of the universe), or in a warm-hot phase with $10^5 < T(\text{K}) < 10^7$ (Davé et al. 2001; Kang et al. 2005; Mo et al. 2005). This gas could have been expelled out of halos by strong winds or never became bound to halos in the first place.

Photoionization of the IGM by quasars or early star formation is an efficient mechanism that impedes gas to fall into small galaxies. Below we estimate the effect that the reionization of the universe could have had on the gas infalling history of NGC 6822.

We use the formulas B1-B3 of appendix B of (Kravtsov, Gnedin, & Klypin 2004) to estimate the effect of reionization on the structure of NGC 6822. The formula B3 given below

$$f_g(M, z) = \frac{f_b}{[1 + 0.26M_F(z)/M]^3}, \quad (10)$$

is an expression for the fraction of cold gas left in the halo of mass M (Gnedin 2000) and f_b is the universal baryon fraction and amounts to 0.14. The filtering mass, M_F , defined as the mass of a halo which would retain 50% of its gas mass, is an increasing function of cosmic time and depends on when reionization starts, z_r (see, for example, Fig. B10 of Kravtsov et al.). We use the mass assembly history $M(z)$ of section 3.3 and equation (10) to compute the fraction of baryonic matter accreted by the galaxy at any given redshift, that is given by

$$f_{acc}(z) = \frac{M(z_r)}{M(z)} f_b + \frac{1}{M(z)} \int_{z_r}^z f_g(M, z) M'(z) dz, \quad (11)$$

where the prime denotes derivative with respect to redshift.

In Figure 2 we plot f_{acc} as a function of time for the mean MAH (solid line). The formula above is formally valid for $z < z_r$, but it is clear that for

redshifts greater than $z_r = 7$ this fraction is just given by f_b . Once the epoch of reionization begins the amount of baryons in the galaxy at any time will depend on how $M_F(z)/M$ evolves. $M_F(z)/M$ varies by about a factor 2 from $z = z_r$ ($t = 0.75$ Gyr) to $z = 0$ ($t = 13.5$ Gyr, the present time) for the MAH model. Its rapid increase from z_r to $z \sim 4$ ($t \sim 5$ Gyr) makes f_{acc} decrease after z_r . As time goes on, the drop in f_{acc} is stopped because $M_F(z)/M$ decreases.

Yet, there is a second mechanism that might reduce the amount of baryons in galaxies: assume that a significant fraction of baryons was never incorporated into the galaxy. Primordial gas could have been shock-heated by the collapse of non-linear structures of mild overdensities (pancakes and filaments), raising the entropy floor (e.g., Mo et al. 2005) and thus increasing the cooling time above the Hubble time. Although simulations with higher numerical resolution are needed to confirm this prediction (Mo et al. 2005), present-day simulations seem to support this idea. Numerical simulations by Kang et al. (2005) show that about 40% of the gas at present is in a warm-hot phase (25% with $10^5 < T(\text{K}) < 10^7$ and 15% with $T(\text{K}) < 10^5$). We will model this phenomena by simply assuming that this increase in temperature in the intergalactic medium occurs suddenly, when the mass of the gas in the galaxy reaches 60% of its present-day value (in the absence of large-scale shock heating). From this epoch, $z = 1.10$ ($t = 5.37$ Gyr), to the present the amount of accreted baryons in the galaxy does not increase. The second drop in f_{acc} (see Figure 2, dotted line) is due to this effect.

It should be clear by now that the evolution of f_{acc} as well as its present-day value depend on the MAH. For the MAHs considered for NGC 6822 and in the absence of large-scale shock heating, $f_{acc}(z = 0)$ takes the following values: 0.033 (slow, $z_f = 1.00$), 0.045 (mean, $z_f = 1.50$), and 0.066 (fast, $z_f = 2.16$). For completeness we also show in Figure 3 the evolution of the total (dashed line) and baryonic (solid line) mass for the mean MAH model, time is cosmic time. As in Figure 2, the dotted line represents the model where the large-scale shock heating of the gas is incorporated.

At this time it may be convenient to summarize the steps we have taken to produce the gas mass accretion history. The infall of gas is propor-

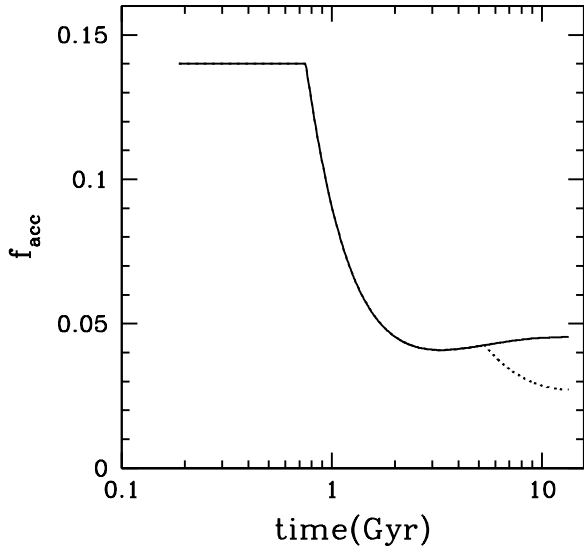


Fig. 2.— Evolution of the ratio of the baryonic matter accreted relative to the total mass for the mean MAH, taking into account the effect of reionization (solid line), and in addition to reionization the effect of large-scale gas shock heating after $t = 5.37$ Gyr (dotted line). Before $t = 5.37$ Gyr the solid line represents both types of models since the effect of large scale shock heating occurs at $t = 5.37$ Gyr and does not affect the MAH for earlier times. We have assumed the onset of reionization at $t_r = 0.75$ Gyr ($z_r = 7$). Note that f_{acc} equals the universal baryon fraction f_b for $t < t_r$ and drops quickly below f_b soon after and reaches a minimum. At $t = 5.37$ Gyr ($z_r = 1.10$), which is the time when the mass gas reaches 60% of the total accreted mass of the large infall models, the curve divides in two: the solid and dotted lines.

tional to that of the dark matter *until the onset* of the reionization epoch which we have taken to be $z = 7$. Once the reionization starts the accretion rate of gas is no longer proportional to that of the dark matter. In fact, in some models, models with shock heating, the fall of gas is stopped while the accretion of dark matter continues. In this sense, the baryonic buildup of the galaxy is not certainly hierarchically. We will see later that the model favored by the observed chemical abundances requires an early galactic wind which in turn makes even less hierarchical the baryonic buildup of NGC 6822. This non hierarchical scenario has been called the downsizing problem and

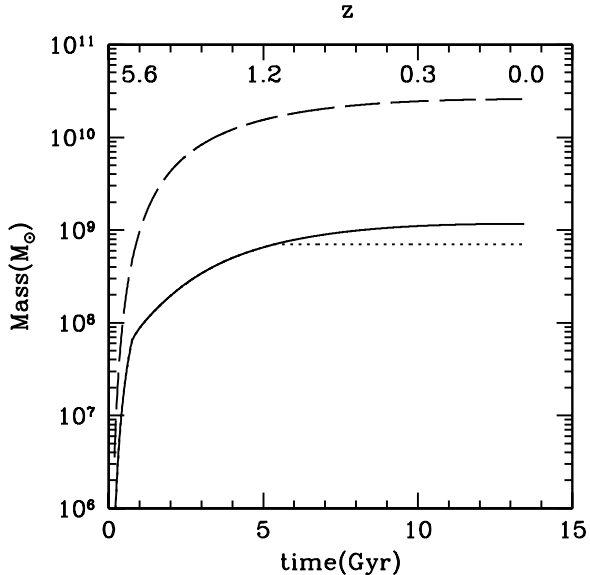


Fig. 3.— Dark (dashed line) and baryonic (solid and dotted lines) mass evolution. The infall of gas follows that of the dark matter until the onset of the reionization of the universe. From then on, the gas mass growth is reduced in relation to that of the DM. After $t = 5.37$ Gyr in the small infall models, in which the intergalactic gas temperature increases due to large-scale shock heating (dotted line), the galaxy stops accreting gas once the gas mass reaches 60% of the total accreted mass of the large infall models (see main text); i. e., in the small infall models we assume that 40% of the gas will never be incorporated into the galaxy.

has been discussed elsewhere (e.g. Arnouts et al. 2005, Cowie et al. 1996).

In section 7 we will describe two families of models for the increase of M_{gas} versus time. Those models that accrete a relatively large M_{gas} and consider the effects of reionization only, will be called *large infall models* (L models), and their chemical evolution will be discussed in section 7.1. Those models that accrete a relatively small M_{gas} and that in addition to reionization consider the effect of shock heating will be called *small infall models* (S models) and will be discussed in section 7.2.

4. Present Mass and Chemical Composition of the Gaseous Component

4.1. Chemical composition

As observational constraints of the evolution models we will use the present chemical composition of the interstellar medium of NGC 6822. To this effect we will combine the abundances of the supergiant stars and the H II regions. The supergiant stars were formed a few million years ago, therefore we expect them to have the same abundances than the H II regions.

In Table 1 we present the adopted NGC 6822 abundances. With the exception of the Fe abundance all the abundances for NGC 6822 are those derived by Peimbert et al. (2005) for Hubble V, the brightest H II region of the galaxy. The Fe abundance was derived by Venn et al. (2001) from two A supergiants and is in excellent agreement with the value derived by Muschelok et al. (1999) from three B supergiants. The gaseous Fe abundance derived from the H II regions can not be used as a constraint because most of the Fe atoms are trapped in dust grains. The O abundance is in very good agreement with the O/H values derived by Venn et al. (2001) for the two A supergiants mentioned before that amount to $12 + \log \text{O/H} = 8.36$.

There has been some discussion about the possible presence of abundance gradients in irregular galaxies, for example Pagel et al. (1978) state that a spatial abundance gradient, an analogous to those found in spiral galaxies, is small or absent in the LMC and conspicuously absent in the SMC. The accuracy of the data on H II regions and supergiant stars for NGC 6822 is not yet good enough to establish the presence of a gradient. Works by Venn & Miller (2002) and Lee et al. (2006) are not conclusive, but seem to indicate that the O/H gradient is small or absent. NGC 6822 V is located about 1 kpc away from the galactic center and according to Gottesman & Weliachew (1977) about 70 % of the gaseous mass ($M(\text{HI}) = 1 \times 10^8 M_{\odot}$) is located within 2.6 kpc. In what follows we will consider that the chemical composition of NGC 6822 V is representative of the gaseous component of NGC 6822.

Also in Table 1 we present the Orion and solar abundances for comparison. For Orion: Fe comes

from B stars (Cunha & Lambert 1994) and the other elements from the H II region (Esteban et al. 2004). The solar abundances come from Asplund et al. (2005), with the exception of the He abundance that corresponds to the initial value computed by Christensen-Dalsgaard (1998).

The Orion nebula is more representative of the present chemical composition of the solar vicinity than the Sun for two main reasons: i) the Sun appears deficient by roughly 0.1 dex in O, Si, Ca, Sc, Ti, Y, Ce, Nd and Eu, compared with its immediate neighbors with similar iron abundances (Allende Prieto et al. 2004), the probable reason for this difference is that the Sun is somewhat older than the comparison stars, and ii) all the chemical evolution models of the Galaxy predict a steady increase of the O/H ratio in the solar vicinity with time, for example the chemical evolution model of the solar vicinity presented by Carigi (2003), Carigi et al. (2005), and Akerman et al. (2004) indicates that the O/H value in the solar vicinity has increased by 0.13 dex since the Sun was formed.

4.2. Gaseous mass: M_{gas}

From the H I measurement by Huchtmeier & Richter (1986) and adopting a distance of 495 kpc we obtain an $M(\text{H I}) = 1.36 \times 10^8 M_{\odot}$. From the helium abundance presented in Table 1 we obtain that $M(\text{He I})/M(\text{H I}) = 0.33$. The $M(\text{H}_2)$ estimated for NGC 6822 by Israel (1997) is about 10 % of $M(\text{H I})$. Consequently, we will multiply the $M(\text{H I}) + M(\text{He I})$ gaseous mass by a factor of 1.1 to take into account the contribution due to $M(\text{H}_2)$. From the previous considerations we obtain that $M_{gas} = (1.98 \pm 0.2) \times 10^8 M_{\odot}$.

5. Luminosity Evolution and Star Formation Rate

5.1. Star formation rate: SFR and its normalization of the M_V

The SFR used in chemical evolution models is given in general by a theoretical parametrization that depends on many physical properties that vary from object to object and in many cases are not well constrained. Consequently, in some cases the adopted SFR might not be realistic. Fortunately for NGC 6822 we have a SFR based on observations.

TABLE 1
NGC 6822, ORION, AND SOLAR TOTAL ABUNDANCES

Element	NGC 6822 ^a	Orion ^b	Sun ^c
12 + log O/H	8.42 ± 0.06	8.73 ± 0.03	8.66 ± 0.05
log C/O	-0.31 ± 0.13	-0.21 ± 0.04	-0.27 ± 0.10
log N/O	-1.37 ± 0.17	-1.00 ± 0.10	-0.88 ± 0.12
log Fe/O	-1.41 ± 0.10	-1.23 ± 0.20	-1.21 ± 0.06
log He/H	10.91 ± 0.01	10.988 ± 0.003	10.98 ± 0.02
Y	0.2433	0.2760	0.2486
Z	0.0066	0.0137	0.0122

^aMuschielok et al. (1999); Venn et al. (2001); Peimbert et al. (2005).

^bCunha & Lambert (1994); Esteban et al. (2004).

^cAsplund et al. (2005); Christensen-Dalsgaard (1998).

Wyder (2001, 2003) based on data obtained with the HST has derived the star formation rate (SFR_i) of eight fields in NGC 6822. Since these 8 fields correspond to regions of the galaxy with different luminosities and taken together amount to 20% of the total luminosity of the object (see below), we will assume that they are representative of the whole galaxy during its evolution. Based on the SFR_i s by Wyder we have constructed a SFR of the whole galaxy.

We have to normalize the results by Wyder to the cosmological age adopted by us. Our cosmological model indicates that the galaxy started forming 13.5 Gyr ago, we have assumed a $SFR = 0$ for the first 1.2 Gyr, therefore the oldest stellar population has a representative age of 12.3 Gyr.

Wyder (2001, 2003) only shows the SFH of region VIII for three assumed galactic ages (9, 12 and 15 Gyr), for the other seven regions he only shows the SFH for an age of the galaxy of 15 Gyr (note that for the SFR time increases towards the future, while for the SFH time increases towards the past). In this paper we have assumed that the differences in the SFH between the ages of 12 Gyr and 15 Gyr are small (as it is the case for region VIII), and have taken the sum of the SFH of all the regions for an age of 15 Gyr as representative of the whole galaxy. In addition we have adopted the SFH in the 15 to 7 Gyr age

interval as representative of the 12.3 to 7 Gyr age interval.

The total star formation rate of the eight fields will be called $SFR(t)_{8f}$ and will be given by

$$SFR(t)_{8f} = \sum_{i=1}^8 SFR(t)_i. \quad (12)$$

With the $SFR(t)_{8f}$ and the GALAXEV program of Bruzual and Charlot (2003) we obtain an $M_V = -14.28$ at the present time ($t = 13.5$ Gyr), which implies that the eight HST fields produce 20% of the luminosity of the galaxy ($M_V = -16.10 \pm 0.1$, Hodge 1977). We added to the GALAXEV program an additional subroutine that includes the metallicity evolution, $Z(t)$ (Bruzual, private communication). The $Z(t)$ used by us is given by the average of the [Fe/H] enrichment histories adopted by Wyder (2003 and private communication) under the assumption that [Fe/H] is proportional to the Z value. This $Z(t)$ function will be called $Z_{Wyder}(t)$.

The SFR_{total} was computed from SFH s based on the Wyder code and was normalized based on the Bruzual-Charlot code. Both codes are different, but we think that the procedure used to derive the luminosity evolution is reasonable, because there are many common ingredients between GALAXEV and Wyder's codes. For example:

both codes use the same IMF (Salpeter 1955) in a similar mass range (from $0.1 M_{\odot}$ to $100 - 120 M_{\odot}$), and the same stellar evolutionary isochrones (those of the Padova group dependent on metallicity).

Assuming that the rest of the galaxy behaves as the HST fields observed by Wyder we obtain that

$$SFR_{total}(t) = N_{SFR} \times \sum_{i=1}^8 SFR(t)_i, \quad (13)$$

where N_{SFR} is the normalization constant. For $N_{SFR} = 5$ we obtain $M_V = -16.07$ at the present time in excellent agreement with the observed value ($M_V = -16.10 \pm 0.1$). In Figure 4 we present the SFR_{total} obtained, this SFR_{total} will be assumed in the models.

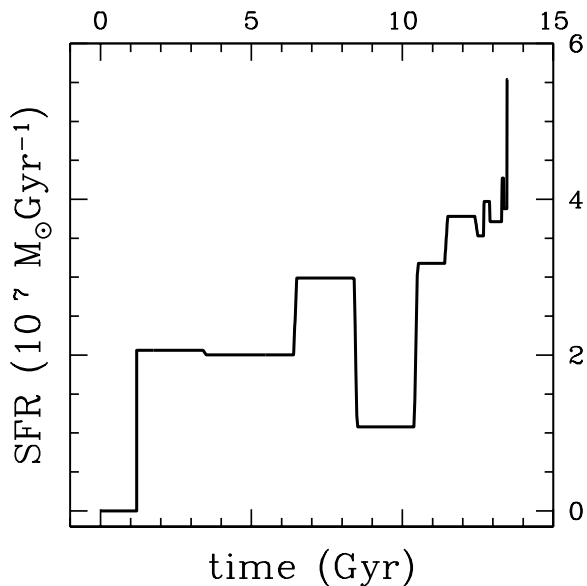


Fig. 4.— Star Formation Rate of NGC 6822 as a function of time determined from the star formation histories of the 8 HST fields.

The M_V was obtained with the GALAXEV code under the assumption of Salpeter IMF and $Z_{Wyder}(t)$.

To reproduce the chemical evolution of the solar vicinity it has been found that the IMF by Kroupa, Tout & Gilmore (1993, KTG) is considerable better than the Salpeter IMF (e.g. Carigi

et al. 2005). Therefore in the next section the chemical evolution models have been computed by adopting the KTG IMF. To test the robustness of the derived the SFR we have computed the M_V value with GALAXEV for the KTG IMF and three different $Z(t)$ functions: $Z_{Wyder}(t)$, $Z(t)$ of model 7L, and $Z(t)$ of model 8S, our two best chemical evolution models (see section 7). For $Z_{Wyder}(t)$, $Z(t)$ of model 7L, and $Z(t)$ of model 8S, we obtained $M_V = -16.22$, $M_V = -16.18$, and $M_V = -16.14$, respectively; these values are within one σ of the observed M_V value, and imply that SFR presented in Figure 4 is robust in changes to the IMF and $Z(t)$ functions.

5.2. Luminosity and color evolution

In Figure 5 and 6 we present the M_U , M_B , and M_V absolute magnitudes evolution and the $J-H$, $J-K$, and $V-J$ colors evolution, respectively, as a function of time for NGC 6822 given by the GALAXEV code with the KTG IMF and $Z(t)$ of model 7L.

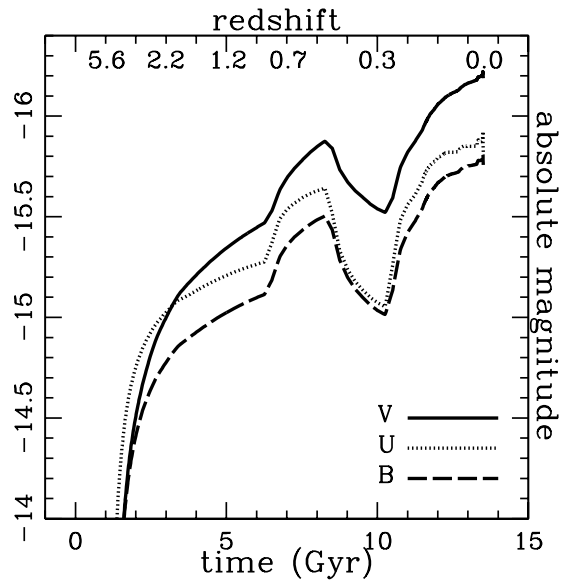


Fig. 5.— U, B, and V absolute magnitudes for NGC 6822 as a function of time. M_U , M_B , and M_V were computed from the SFR shown in Fig. 4 using the GALAXEV code with metallicity evolution of model 7L (our best chemical evolution model) and the KTG IMF.

In Table 2 we compare the observed magnitudes

and colors with those predicted by different models for the present time (13.5 Gyr). The magnitudes M_B and M_V are taken from Wyder (2001), while the colors $M_J - M_H$ and $M_J - M_K$ from Jarret et al. (2003). The $U - B$ color is from Hodge (1977) and the reddening correction for $U - B$ was taken from Schlegel et al. (1998). The agreement between the model predictions and observations is excellent for the M_U , M_B , and M_V magnitudes and the $M_J - M_H$ and $M_J - M_K$ color indexes (see also Figure 6).

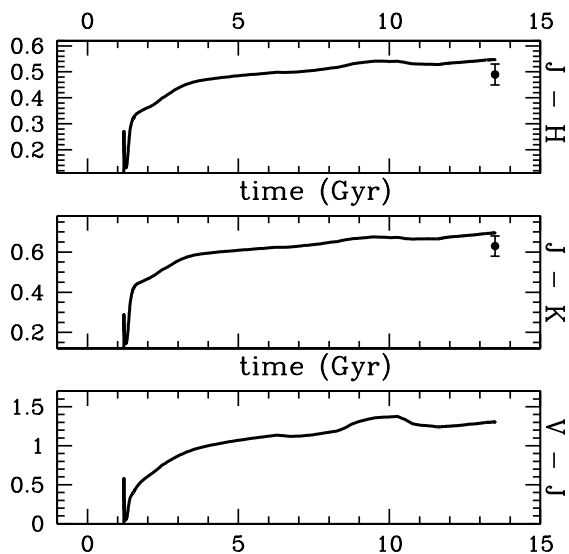


Fig. 6.— Same as Fig 5, but for the $J - H$, $J - K$, and $V - J$ colors. The observational constraints $M_J - M_H$ and $M_J - M_K$ are also presented for comparison (Jarret et al. 2003).

It is not possible to compare the visual magnitudes with the infrared magnitudes because the infrared observations did not include the whole galaxy (Jarrett et al. 2003). By adopting the $M_V - M_J$ color of the $Z(t)$ 7L model, we can determine the fraction of the integrated light of the galaxy observed in the infrared. The photometric evolution model predicts $M_V - M_J = 1.32$ and $M_J = -17.50$. On the other hand the observed M_J value by Jarrett et al. (2003) amounts to -16.2 a value 1.3 mag fainter than predicted by the model. This difference implies that the aperture used by Jarrett et al. (2003) included only 30 % of the integrated light of the galaxy, in agreement with the comment in their section 6.5 where

they mention that in general they observed only from 20 % to 50 % of the integrated light of dwarf irregular galaxies.

From Table 2 it can be seen that the different models agree with the observations at one σ level. In other words the absolute luminosity in different bands as well as the color indexes are almost independent of the three different $Z(t)$ functions as well as the two IMF's used and consequently that the SFR presented in Fig. 4 is robust and can be used for all the chemical evolution models. That is the SFR has been derived from observations and it will be kept fixed for all the chemical evolution models.

6. Galactic Winds

A common hypothesis in chemical evolution models of dwarf galaxies is to assume that these galaxies expelled part of their gas during their lifetime: a galactic wind is mostly introduced in the modelling to explain the low chemical abundances found in these type of galaxies and NGC 6822 seems to be no exception. From an observational point of view the amount of evidence of outflows in star forming galaxies is increasing with time and we refer the reader to Veilleux et al. (2005) for an updated discussion of galactic winds. On the other hand, from a theoretical point of view, numerical simulations show that a blow-away outflow situation is not rather uncommon phenomenon in low-mass galaxies (e.g Fujita et al. 2004).

In order to see if NGC 6822 could have had a galactic wind during its lifetime, specially at high redshift, we have computed its present date binding energy as well as the thermal energy history of the gas. In Figure 7 we present the thermal energy of the gas as a function of time assuming no outflows.

The thermal energy was computed as follows: we define E_{THER} as the thermal energy of the gas from supernovae,

$$E_{THER}(t) = \int_0^t \epsilon(t - T) RSN(T) dT \quad (14)$$

where RSN is the supernovae rate and includes types Ia and II SNe. The $\epsilon(t)$ function represents the evolution of the thermal energy in the hot, dilute interior of the supernovae remnants and is given by

TABLE 2
PRESENT-DAY PHOTOMETRIC PROPERTIES FOR DIFFERENT INITIAL MASS FUCTIONS AND METALLICITY EVOLUTIONS

IMF $Z(t)$	Salpeter Wyder	KTG Wyder	KTG Model 7L	KTG Model 8S	Observations
M_U	-15.97	-15.91	-15.82	-15.74	-15.83 ± 0.16
M_B	-15.74	-15.81	-15.76	-15.70	-15.60 ± 0.13
M_V	-16.07	-16.22	-16.18	-16.14	-16.10 ± 0.10
$M_J - M_H$	0.52	0.53	0.55	0.56	0.49 ± 0.04
$M_J - M_K$	0.66	0.66	0.70	0.72	0.63 ± 0.05
$M_V - M_J$	1.18	1.26	1.32	1.35	—
Z_{NOW}	0.0024	0.0024	0.0069	0.0084	0.0066 ± 0.0011

$$\epsilon(t) = \begin{cases} 0.72\epsilon_0 & \text{if } t \leq t_C, \\ 0.22\epsilon_0(t/t_C)^{-0.62} & \text{if } t > t_C, \end{cases}$$

where $\epsilon_0 = 10^{51}$ erg and t_C is a cooling time scale taken from Cox (1972). For further details see Carigi, Hernández & Gilmore (2002).

Also in Fig. 7 we show the binding energy of NGC 6822 for the present gas content based on the following equation:

$$E_{BIND} = G \frac{M_{gas} M_{total}}{R_{vir}}. \quad (15)$$

As can be seen from Figure 7 the thermal energy available, released during the lifetime of the galaxy, is higher than the present binding energy of the gaseous content of the galaxy, which implies that part of the thermal energy was lost by the galaxy in the past. This result is in agreement with the chemical evolution models that require a substantial gas outflow to match the present gaseous content with the observed O/H value (see section 7).

As we mention above, the computation of the thermal energy content of NGC 6822 is based on the cooling scheme by Cox (1972). A more elaborated treatment of the SN remnant cooling has been presented by Tantalo et al. (1998). They computed the cooling time as a function of gas metallicity and found that for metallicities below solar it is larger than that predicted by Cox. Thus,

in absence of winds, the thermal energy in NGC 6822 should lie above the one shown in Fig. 7.

The outflows needed to explain the excess thermal energy predicted by the observed SFR and by the chemical evolution model presented in section 6 very likely occurred in the first few Gyr of evolution ($t < 5$ Gyr) because: i) To propitiate an efficient blow away process strong bursts of star formation are needed (Tenorio-Tagle et al. 2003), from the SFR it is not possible to rule out the presence of several outburst processes at early times ($t < 5$ Gyr), because the SFR has been averaged at long time intervals (~ 2.5 Gyr), and it is possible for one or two large bursts of star formation, to go unnoticed in the derived SFR , on the other hand, at later times the SFR has been averaged for shorter time intervals (~ 0.5 Gyr), and it is more difficult for a high SFR to go unnoticed; ii) in the past, in a hierarchical cosmology, the potential wells of galaxies, for a given present-day mass, are shallower; iii) strong star formation events are expected to occur because of the higher galaxy merger rate (e.g., Maller et al. 2005); iv) after an outflow occurs, M_{gas} gets diminished and the possibility of a second outflow due to a burst of star formation increases because there is a lower amount of gas in the ISM to reduce the velocity of the SN ejecta, and v) the low metallicity at early times increases the cooling time relative to the classical Cox (1972) value, and therefore increases the thermal energy available propitiating

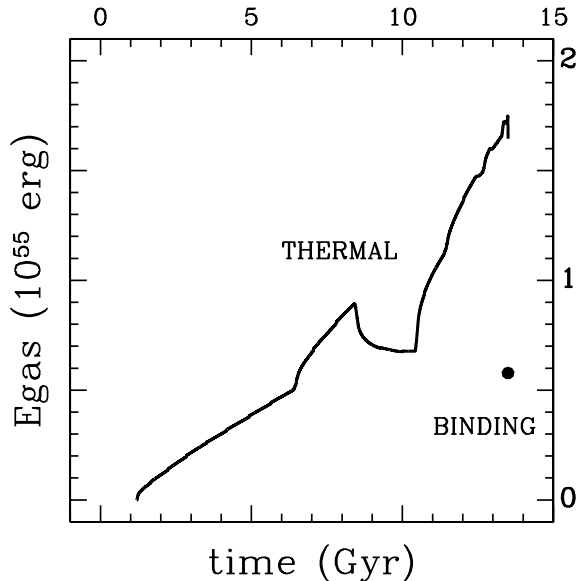


Fig. 7.— Gaseous thermal energy predicted by SFR under the assumption of no gaseous outflow from the galaxy based on the formulation by Cox (1972). We also show the binding energy of the present gas content of the galaxy. The difference between the predicted thermal energy and the binding energy at present implies that the galaxy must have lost thermal energy due to outflows in the past.

the advent of galactic winds. As can be seen from our chemical evolution models, for example models 7L and 8S (see section 7) the Z value for $t < 5$ Gyr is about 0.001, thirteen times smaller than solar.

It is beyond the scope of this paper to study the outflow rate as a function of time.

7. Chemical Evolution Models

We have computed chemical evolution models with a very low number of free parameters. The cosmological context provides the accretion rate, and the luminosity model provides the SFR as a function of time, both in an independent way. The remaining ingredients related with stellar populations: the IMF, the stellar yields, and the percentage of binary systems which explode as SNIa, are inferred from a successful chemical evolution model of the solar vicinity and the Galactic disk by Carigi et al. (2005).

To construct the models for NGC 6822, we have relied upon the model of the solar vicinity by Carigi et al. (2005), consequently we have adopted the following assumptions: i) the IMF proposed by Kroupa, Tout, & Gilmore (1993, KTG) for the 0.01 - 80 M_{\odot} range, ii) for massive stars, those with $m > 8 M_{\odot}$, we have used yields that depend on the initial metallicity as follows, for $Z_i = 0$ yields by Chieffi & Limongi (2002), for $Z_i = 1 \times 10^{-5}$ and 0.004 yields by Meynet & Maeder (2002), and for $Z_i = 0.02$ yields by Maeder (1992), iii) for low-and-intermediate-mass stars, those with $m < 8 M_{\odot}$ and from $Z_i = 0.004$ to $Z_i = 0.02$ we have used the yields by Marigo, Bressan, & Chiosi (1996, 1998), and Portinari et al. (1998), iv) for Type Ia supernovae, we have used the yields for $Z_i = 0.02$ by Thielemann et al. (1993), these yields are almost independent of metallicity, and v) the fraction of binary systems with total mass between $3 < m(M_{\odot}) < 16$ that becomes SNIa (*Abin*) amounts to 0.05. For each set of yields, linear interpolations for different stellar masses and metallicities were made. For metallicities higher or lower than those available we adopted the yields predicted by the highest or lowest Z available, respectively.

In some models, we will adopt two different types of outflows: i) we call “selective outflows” those constituted only by material ejected by supernovae of Type II and Type Ia, in this case all the material ejected by massive stars (Type II SNe) is lost to the IGM, and ii) we call “well mixed outflows” those that reach the IGM after the ejecta by MS, LIMS, and Type Ia SNe have been completely mixed with the ambient ISM. We have assumed that the rate of the well mixed outflow is proportional to the SFR and that the proportionality coefficient is constant during the presence of the outflow. With both types of outflows the galaxy loses material that never gets back. The duration of the outflow is another free parameter.

We computed a large set of chemical evolution models. From these, we will discuss in detail 15 models in sections 7.1 and 7.2. All models evolve with the mean MAH computed in section 3.3. Seven of the 15 models follow a baryonic mass accretion history that does not assume large-scale heating of the gas, while the other eight models do. In some models we included outflows of baryonic

matter. All models fit the observed colors evolution in Section 5.2, and twelve of them have the same values for M_{sub} , M_{stars} , and M_{rem} , at the present time, these values amount to $3.48 \times 10^7 M_{\odot}$, $1.73 \times 10^8 M_{\odot}$, and $2.31 \times 10^7 M_{\odot}$. The exceptions are Model 7L, 7S, and 8S, that have different upper mass limits for the IMF, for these models the values of M_{sub} , M_{stars} , and M_{rem} are practically the same values than those predicted by the other models and they will be presented in sections 6.1 and 6.2. The M_{bar} determined from the observed gaseous mass and the other terms present in eq. 2 amounts to $4.3 \times 10^8 M_{\odot}$.

7.1. Large infall models

We have computed several models that adopt all the ingredients presented in the previous sections, specially in Sections 3, 5.1 and 7. In particular, in Models 1L – 7L we consider that the baryonic mass accreted by NGC 6822 is that suggested by the cosmological context without large-scale shock heating.

In Table 3 we present the main characteristics of seven models. Columns 2 and 3 describe the type of outflow and its duration. Columns 4 to 8 present five properties predicted by the models: M_{gas} , O/H, C/O, N/O, and Fe/O, as well as their observed values. The M_{gas} and the O/H values are the most critical observational constraints for NGC 6822, therefore a model that fits the C/O, N/O and Fe/O observed values, but that does not fit the observed O/H value, is a poor model because it does not fit the C/H, N/H, and Fe/H observed values.

In Model 1L we assume that all the baryons available after the reionization fall into the galaxy and remain in the galaxy during its whole evolution. In Figure 8 we show the evolution history of six properties of the model up to now. Model 1L grossly fails to fit M_{gas} and O/H, since it predicts 4.7 times more gas than observed and a lower O/H value than observed by 5σ (see Table 3 and Figure 8).

In order to reduce the enormous difference between the predicted M_{gas} value by Model 1L and the observed value we have computed models with well mixed outflows during the early history of the galaxy.

Model 2L is built to reproduce the M_{gas} ob-

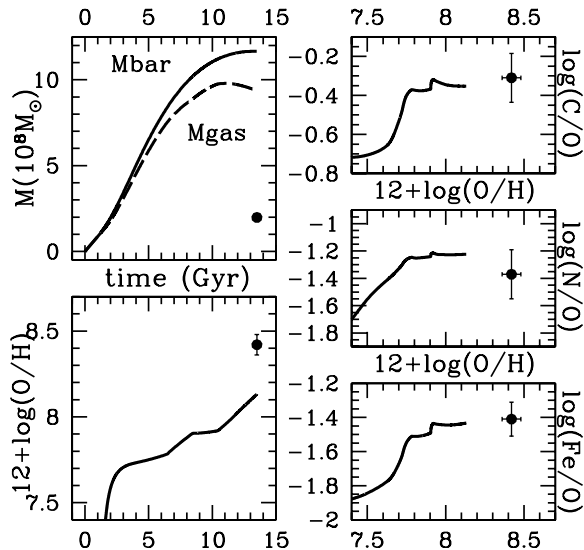


Fig. 8.— Model 1L. Mass formation history and predicted chemical evolution. This model assumes that all the gas available after the reionization falls into the galaxy and does not include outflows. The present-day observational constraints (filled circles) are also presented for comparison. The model fails drastically.

served value under the assumption of an instantaneous well mixed outflow. This event had to occur at 6.3 Gyr, because at that time the M_{gas} of the galaxy amounts to the difference between the observed and the predicted M_{gas} by Model 1L ($7.38 \times 10^8 M_{\odot}$). This model reproduces M_{gas} , C/O and Fe/O, but the O/H and N/O values are higher than observed by 2.0σ and 1.2σ respectively (see Table 3). O/H is higher because according to the *SFR* most of the stars are formed after the outflow event and the O ejected by the stars to the ISM is kept by the galaxy

Based on the models by Fujita et al. (2004) we find that in order to produce an instantaneous well mixed wind in NGC 6822 at 6.3 Gyr, when its total mass is $1.7 \times 10^{10} M_{\odot}$, about 10% of the gas should be converted into stars. This amount of gas corresponds to $\sim 6 \times 10^7 M_{\odot}$ which according to the derived *SFR* is 2.5 times higher than the mass converted into stars by NGC 6822 in an interval of 1 Gyr centered at 5.8 Gyr (see Figure 4). Consequently, we consider Model 2L to be un-

likely.

Model 3L is built to reproduce the O/H observed value under the assumption of a well mixed outflow that starts at the same time than the star formation ($t = 1.2$ Gyr). To reproduce the observed O/H value the model needs the outflow phase to last 4.0 Gyr. During the outflow phase the mass lost to the IGM is the maximum possible, that means that the gas left is the minimum required to maintain the SFR given in Fig. 4.

Model 3L reproduces all the observational constraints related with chemical abundances, but not the M_{gas} observed value: the M_{gas} predicted is higher than observed, by a factor of 1.65 (8σ) (see Table 3 and Figure 9). The gas mass lost is $6.09 \times 10^8 M_{\odot}$, 8.5 times the mass of stars formed during the first 4.0 Gyr. During the wind phase the outflow rate is equal to 7.51 times the SFR . If it turns out that the observed gas mass value has been underestimated (which is unlikely since most of the gas is in the form of HI that is observed), this model might become relevant.

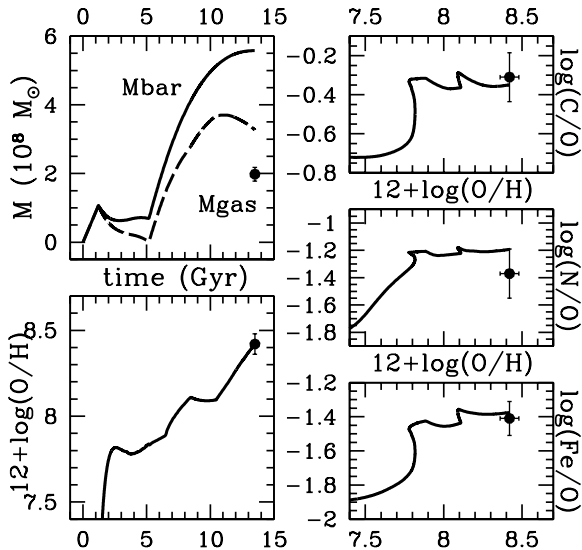


Fig. 9.— Model 3L. Mass formation history and predicted chemical evolution. This model assumes the gas mass assembly history of the large infall models and includes a well mixed outflow during the first 4 Gyr of the star formation.

Model 4L is built to reproduce the M_{gas} observed value under the assumption of a well mixed

outflow. This model requires to lose more gas than Model 3L, therefore the duration of the outflow has to be longer. To fit M_{gas} we need the outflow to last 5.1 Gyr. During the outflow phase the mass lost to the IGM is the maximum possible, that means that the gas left is the minimum required to maintain the SFR . During the wind phase the outflow rate is equal to 7.11 times the SFR . The gas mass lost is $7.35 \times 10^8 M_{\odot}$, 8.0 times the mass of stars formed during the first 5.1 Gyr of the star formation. The predictions of this model are identical to those of Model 2L (see Table 3), from ~ 7 Gyr up to now, because: i) both models at ~ 5 Gyr had lost practically all of the gas and started accumulating gas again at the same rate, and ii) both models had the the same SFR after 5 Gyr. In other words, after the end of the outflow phase both models have the same stellar populations that pollute equally the same amount of gas.

Model 4L agrees with the observed M_{gas} value but overproduces O, therefore we will modify Model 4L to fit the O/H ratio and the other observational constraints by adopting extra assumptions in Models 5L, 6L, and 7L.

In Model 5L we have assumed that 0.5 Gyr ago a primordial gaseous cloud of $0.34 \times 10^8 M_{\odot}$ was accreted by NGC 6822. We have assumed the least massive cloud needed to reproduce the O/H value. With this extra infall, the model can reproduce all the observational constraints related to chemical abundances with the exception of N/O, but the predicted M_{gas} is higher by a factor of 1.2 (see Table 3). The accretion of a huge gaseous cloud of primordial material recently is more unlikely than at earlier times. If we assume the accretion of a primordial cloud at earlier times ($t < 13$ Gyr), the model would require a more massive cloud, increasing the disagreement with the observed M_{gas} .

To assume the infall of a cloud of $3.4 \times 10^7 M_{\odot}$ of primordial gas at $t = 13$ Gyr is unlikely for the following reasons: i) this gaseous cloud has about 8 % of the baryonic mass of the galaxy and therefore could have formed part of the NGC 6822 satellite system, ii) at such late time a gas cloud of this mass could have had time to form stars and these stars could have changed the primordial chemical composition of the gas cloud (according to De Block & Walter (2005) the disk of NGC 6822 does have an embedded gaseous cloud with comparable

mass but with an old stellar population), and iii) the total gaseous mass accreted by the galaxy in the last 0.5 Gyr according to the MAH amounts only to $5 \times 10^5 M_\odot$. Consequently, we consider Model 5L unlikely.

In Model 6L we have assumed a second outflow of the selective type, during the last 1 Gyr, when the *SFR* is most important. In this outflow, all the material ejected by SNIi and SNIa is lost to the IGM. If the SNIa ejecta remain in the galaxy, the predicted Fe/O value becomes -1.30 dex, in marginally agreement with observations (see Table 3). Model 6L is unlikely because between 12.5 and 13.5 Gyr the *SFR* does not indicate the presence of a major starburst (see Figure 4) needed to drive the outflow, and the potential gravitational well is largest. Moreover, we think that it is unlikely that the material ejected by every SNe in the last Gyr escapes to the IGM.

In Model 7L we have reduced the IMF mass upper limit, m_{up} , from $80 M_\odot$ to $60 M_\odot$. When m_{up} is reduced, the percentage of MS, main producers of O, is decreased by a factor of 1.18, and the predicted O/H value is reduced by 0.12 dex. This fact produces an increase of the N/O and Fe/O predicted values to -1.06 dex and -1.24 dex, respectively, more than 1σ away from the observed values. The Fe/O value can be adjusted by assuming a lower fraction of binary systems that become SNIa (*Abin*). For this reason we have reduced *Abin* from 0.05 (the value assumed in the rest of the L models) to 0.02. Model 7L fits all the observational constraints with the exception of the N/O ratio (see Figure 10 and Table 3).

With $m_{up} = 60 M_\odot$, and *Abin* = 0.02, the stellar populations are not the same than those in the solar vicinity. With these values the model by Akerman et al. (2005) or Carigi et al. (2005) cannot reproduce the chemical observational constraints for the solar vicinity, implying that the IMF's of the solar vicinity and of NGC 6822 are not the same. Other authors have also argued in favor of smaller m_{up} values for dwarf galaxies, for example, Weidner & Kroupa (2005) suggest that m_{up} is lower in dwarf galaxies than in the solar vicinity; the smaller m_{up} implies that the number of Type II SN per generation of stars has to be smaller than in the solar vicinity. Their results depend on the *SFR*. For a continuous *SFR* during the last 14 Gyr, their IMF slope is steeper

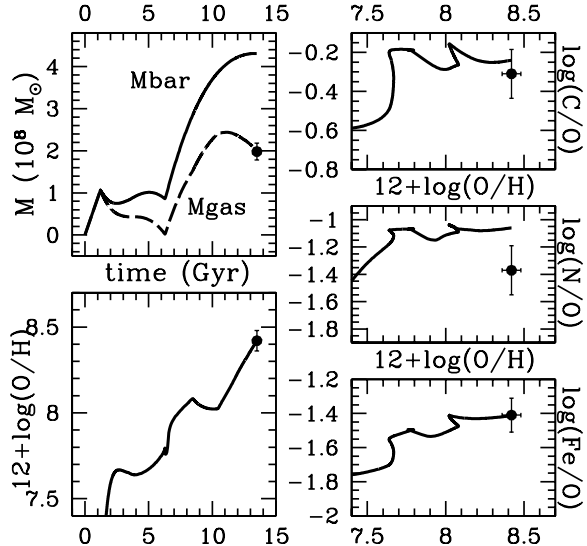


Fig. 10.— Model 7L. Mass formation history and predicted chemical evolution. This model assumes the gas mass assembly history of the large infall models and includes a well mixed outflow during the initial 5.1 Gyr of the star formation. The IMF $m_{up} = 60 M_\odot$, and the fraction of binary systems that becomes SNIa is 2 %.

than the Salpeter IMF for massive stars, as in the case of the IMF assumed in this paper, and has an $m_{up} \sim 10 M_\odot$. For a single 100 Myr burst their slope is like the Salpeter's one and has an $m_{up} \sim 100 M_\odot$. The *SFR* computed by us is nearly constant during the first 5 Gyr and then shows several bursts. Based on the work by Weidner & Kroupa the IMF adopted by us should be dependent on time, but that is out of the scope of this paper. We consider that a constant IMF with $m_{up} = 60 M_\odot$ is a good approximation to the IMF proposed by Weidner & Kroupa (2005). Other authors also argue that galaxies with a lower *SFR* have a lower m_{up} value in agreement with our suggestion (e.g. Goodwin & Pagel 2005, and references therein).

The change in m_{up} from $80 M_\odot$ to $60 M_\odot$ affects the O/H evolution, but it does not affect the photometric evolution nor the thermal evolution. We have computed a photometric evolution model with $m_{up} = 60 M_\odot$ and obtained $M_U = -15.82$, $M_B = -15.77$, $M_V = -16.19$, $M_J - M_H = 0.55$, $M_J - M_K = 0.70$, and $M_V - M_J = 1.32$ practi-

TABLE 3
 INPUTS AND OUTPUTS OF LARGE INFALL MODELS

Model	Wind		M_{gas} ($108 M_{\odot}$)	$12+\log(\text{O}/\text{H})$	Abundances		
	Type	Duration (Gyr)			$\log(\text{C}/\text{O})$	$\log(\text{N}/\text{O})$	$\log(\text{Fe}/\text{O})$
1L	—	—	9.36	8.13	-0.35	-1.22	-1.43
2L	Well Mixed	0.1	1.99	8.54	-0.33	-1.16	-1.35
3L	Well Mixed	4.0	3.27	8.42	-0.35	-1.19	-1.38
4L	Well Mixed	5.1	2.01	8.54	-0.33	-1.16	-1.35
5L ^a	Well Mixed	5.1	2.34	8.48	-0.34	-1.17	-1.35
6L ^b	Well Mixed	5.1	1.98	8.42	-0.27	-1.09	-1.37
7L ^c	Well Mixed	5.1	2.01	8.42	-0.24	-1.06	-1.41
Obs.			1.98 ± 0.20	8.42 ± 0.06	-0.31 ± 0.12	-1.37 ± 0.18	-1.41 ± 0.10

^aExtra $3.4 \times 10^7 M_{\odot}$ of primordial gas accreted at 13.0 Gyr.

^bAll the material expelled by Type II and Ia SNe during the last Gyr is ejected to the IGM.

^cThe upper mass limit for the IMF amounts to $60 M_{\odot}$. The fraction of binary systems that become SNIa amounts to 0.02.

cally identical to those derived with $m_{up} = 80 M_{\odot}$ presented in Table 2, therefore the change in the SFR due to the reduction of m_{up} from $80 M_{\odot}$ to $60 M_{\odot}$ is negligible. Similarly, the gaseous thermal energy produced by the SFR under the assumption of no outflows diminishes from 1.65×10^{55} erg to 1.63×10^{55} erg when m_{up} changes from 80 to $60 M_{\odot}$.

For Model 7L the current values of M_{sub} , M_{stars} , and M_{rem} , amount to $3.49 \times 10^7 M_{\odot}$, $1.73 \times 10^8 M_{\odot}$, and $2.31 \times 10^7 M_{\odot}$, respectively.

It can be shown that the use of the Salpeter IMF would imply a smaller m_{up} than that required by KTG IMF to fit the observed O/H value. Consequently, since all of the O is produced by massive stars and only a fraction of the C is produced by them, the C/O value would become considerably larger than observed (e.g. see model 7S).

In Table 4 we present two carbon budgets: the stellar production one, and the interstellar medium one for L models. The production is due to massive stars (MS), low and intermediate mass stars (LIMS), and SNIa. Also in Table 4 we present for comparison the carbon budgets for the solar vicinity (Carigi et al. 2005). For Model 1L both budgets agree because there is no outflow present, a similar situation prevails for the solar vicinity. For Models 4L, 6L, and 7L the contribution of massive stars to the C abundances in the ISM is smaller than the stellar production due to outflows to the IGM. Since for Models 4L and 6L the IMF and the SFR are the same, the higher contribution of MS to the C budget is due to the dependence of the C yields in the O/H ratio, which is higher for Model 4L than for Model 6L. For MS the C yields increase with metallicity due to stellar winds, while for LIMS the C yields decrease with metallicity (Carigi et al. 2005). Since for Models 6L and 7L the SFR and the O/H values are the same, the higher contribution of MS to the C budget is due to the difference in the IMFs, while for Model 6L m_{up} amounts to $80 M_{\odot}$ for Model 7L it only amounts to $60 M_{\odot}$. Finally the larger contribution of MS to the C budget in the solar vicinity than in Model 1L is due to the evolution of the O/H values, and as mentioned before the higher O/H values produce higher C yields for MS and lower ones for LIMS.

The difference among the carbon budgets of the computed models for NGC 6822 is small and im-

plies that the result obtained, in the sense that the LIMS produce about 63 % of the C abundance and that the MS produce about 36 % of the C abundance, is a robust one.

7.2. Small infall models

For the S models we consider the baryonic mass aggregation history obtained in section 3.4 under the assumption of large-scale gas shock heating, that prevents a fraction of the gas to be accreted by the galaxy. Specifically, only 60 % of the baryons available after taking into account the effect of reionization (see Figures 2 and 3, dotted lines) fall into the galaxy. The remaining 40 % of the baryons are heated by the collapse of large-scale structures (filaments and pancakes) and are never accreted by the galaxy.

In Table 5 we present the main characteristics of eight S models. Columns 2 and 3 describe the type of outflow and its duration. Columns 4 to 8 present five properties predicted by the models.

In Model 1S we assume that the gas that falls into the galaxy remains in the galaxy during its whole evolution. In Figure 11 we show the evolution history of six properties of the model up to the present time. Model 1S fails to fit M_{gas} , since it predicts 2.4 times more gas than observed, but reproduces all the observational constraints related with chemical abundances (see Table 5 and Figure 11). If the observed M_{gas} value were higher than the adopted in this paper, this model would be one of the best and would be the only successful model without outflow.

In order to reduce the difference between the predicted and observed M_{gas} presented by Model 1S we have computed models that include well-mixed outflows during the early history of the galaxy.

Model 2S is built to reproduce the observed M_{gas} under the assumption of an instantaneous well mixed outflow. This event had to occur at 3.1 Gyr, because at that time the M_{gas} of the galaxy amounts to the difference between the observed and the predicted M_{gas} by Model 1S ($2.73 \times 10^8 M_{\odot}$). This model reproduces M_{gas} but the O/H value is higher than observed by 3.7σ (see Table 5). The C/H, N/H and Fe/H ratios are not reproduced.

Model 3S is built to reproduce the O/H ob-

TABLE 4
CARBON BUDGET FOR LARGE INFALL MODELS^a

Model	Contribution (per cent)		
	MS	LIMS	SNIa
1L	36.3	61.4	2.3
4L	38.2	59.5	2.3
6L	37.7	60.1	2.3
7L	35.9	63.2	0.9
Solar Vicinity	48.2	49.8	2.0
Remaining values in the ISM			
1L	36.3	61.4	2.3
4L	37.2	60.4	2.4
6L	30.8	67.1	2.1
7L	34.2	64.8	1.0
Solar Vicinity	48.2	49.8	2.0

^aPercentage of C in the ISM produced by different types of stars over a period of 13 Gyr.

served value under the assumption of a well mixed outflow that starts at the same time than the star formation. To reproduce the observed O/H value the outflow phase has to last only 0.1 Gyr. This model is very similar to Model 1S. During the wind phase the outflow rate is equal to 10.0 times the *SFR*. This model reproduces all the observational constraints related with chemical abundances, but not the M_{gas} observed value (see Table 5).

Model 4S is built to reproduce M_{gas} value under the assumption of an early well mixed outflow that lasts 1.6 Gyr. Since Model 4S accretes less gas than Model 4L, it requires an outflow during a shorter amount of time to reproduce the M_{gas} observed. During the outflow phase the mass lost to the IGM is the maximum possible, that means that the gas left is the minimum required to maintain the *SFR*.

During the wind phase the outflow rate of Model 4S is equal to 8.56 times the *SFR*. The gas mass lost in the outflow amounts to $2.73 \times 10^8 M_{\odot}$, 9.5 times the mass of stars formed during the first 1.6 Gyr of the star formation. The predictions of this model are identical to those of Model 2S (see Table 5), from ~ 3 Gyr up to now, because

both models at ~ 3 Gyr had lost practically all of their gas and started accumulating gas again at the same rate and with the the same *SFR* during their later evolution. In other words, after the end of the outflow phase both models have the same stellar populations that pollute equally the same amount of gas.

In Model 4S accretion stops after 5 Gyr, when the *SFR* is important. Therefore, its predicted O/H value is higher than that obtained by Model 4L because the chemical elements produced by the stars after $t= 2.8$ Gyr are ejected into an ISM which is no longer diluted by primordial infalling gas. To lower the O/H value of Model 4S we have produced Models 5S – 7S that require even more extreme extra assumptions than those needed for Models 5L – 7L.

In Model 5S in order to reproduce the O/H value with the least massive cloud we have assumed that 0.5 Gyr ago a primordial gaseous cloud of $1.2 \times 10^8 M_{\odot}$ was captured by NGC 6822. With this extra infall, the model can reproduce all the observational constraints related to chemical abundances with the exception of N/O, but the predicted M_{gas} is higher by a factor of 1.6 (see Ta-

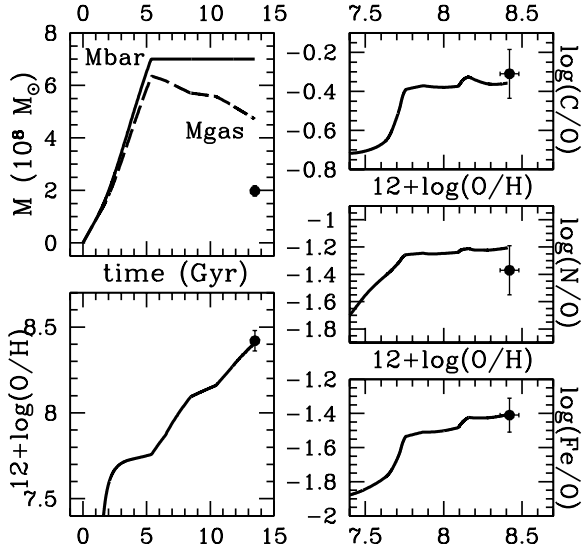


Fig. 11.— Model 1S. Mass formation history and predicted chemical evolution. This model assumes that 40 % of the gas available after the reionization does not fall into the galaxy and this model does not include outflows. The present-day observational constraints are also presented for comparison. The model fails to reproduce M_{gas} .

ble 5). The accretion of a huge gaseous cloud of primordial material recently is more unlikely than at earlier times. If we assume an accretion of a primordial cloud at $t < 13$ Gyr, with the same SFR (important at recent times), the model will require a more massive cloud producing a larger disagreement with the observed M_{gas} . We consider Model 5S more unlikely than Model 5L because the mass of the infalling cloud has to be larger and the disagreement with the observed M_{gas} becomes also larger.

For Model 6S we have assumed a second outflow of the selective type during the last 2.5 Gyr, when the SFR is most important. In this outflow, 100 % of the material ejected by all SNI and SNIa is lost to the IGM. This model predicts higher C/O and N/O values (see Table 5) because the galaxy keeps the C and N produced by LIMS. Model 6S is unlikely because between 11.0 and 13.5 Gyr the SFR does not indicate the presence of a major starburst (see Figure 4) needed to drive the outflow, and the potential gravitational well is largest. Moreover,

Model 6S is more unlikely than Model 6L because it requires a recent rich outflow of longer duration.

In Model 7S we have reduced m_{up} from $80 M_{\odot}$ to $47 M_{\odot}$ and consequently the predicted O/H value is reduced by 0.22 dex. This fact produces an increase of the C/O and N/O predicted values to -0.12 dex and -0.93 dex, respectively, more than 1.5σ away from the observed values (see Table 5). The Fe/O value is adjusted because we have assumed a lower fraction of binary systems that become SNIa ($A_{bin} = 0.02$). This model does not reproduce the C/O and N/O values because with this IMF there are more LIMS that are the main producers of C and N, at these metallicities. For Model 7S the values of M_{sub} , M_{stars} , and M_{rem} , amount to $3.50 \times 10^7 M_{\odot}$, $1.72 \times 10^8 M_{\odot}$, and $2.30 \times 10^7 M_{\odot}$, respectively.

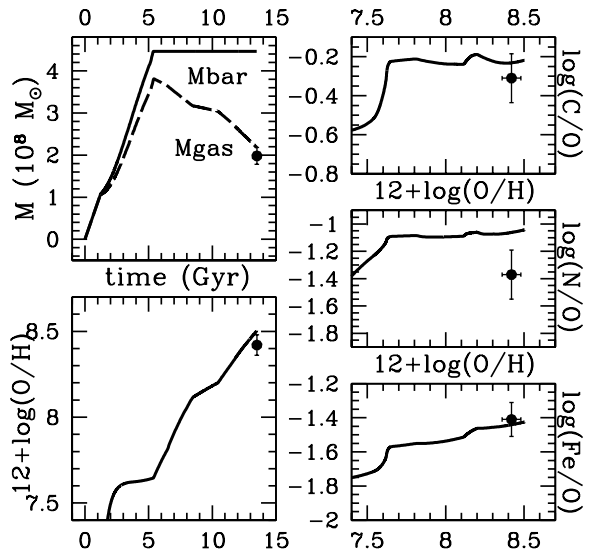


Fig. 12.— Model 8S. Mass formation history and predicted chemical evolution. This model assumes the gas mass assembly history of small infall model and includes a well mixed outflow during the initial 4.0 Gyr of the star formation. The IMF m_{up} is set to $60 M_{\odot}$ and the fraction of binary systems that becomes SNIa is 2 %.

No previous S model reproduces all the observational constraints. In particular, those models that match M_{gas} , predict higher O/H values than observed. The extra assumptions included in the models produce a rise in the C/O value, higher than observed. Consequently, we have computed

TABLE 5
 INPUTS AND OUTPUTS OF SMALL INFALL MODELS

Model	Wind Type	Wind Duration (Gyr)	M_{gas} (108 M_{\odot})	$12+\log(O/H)$	Abundances		
					$\log(C/O)$	$\log(N/O)$	$\log(Fe/O)$
1S	—	—	4.71	8.41	-0.36	-1.21	-1.41
2S	Well Mixed	0.1	1.99	8.64	-0.29	-1.13	-1.35
3S	Well Mixed	0.1	4.51	8.42	-0.36	-1.20	-1.41
4S	Well Mixed	1.6	1.98	8.64	-0.29	-1.13	-1.35
5S ^a	Well Mixed	1.6	3.18	8.48	-0.30	-1.14	-1.36
6S ^b	Well Mixed	1.6	1.92	8.42	-0.18	-0.99	-1.38
7S ^c	Well Mixed	1.6	1.98	8.42	-0.12	-0.93	-1.31
8S ^d	Well Mixed	4.0	2.18	8.50	-0.22	-1.04	-1.43
Obs.			1.98 ± 0.20	8.42 ± 0.06	-0.31 ± 0.12	-1.37 ± 0.18	-1.41 ± 0.10

^aExtra $1.2 \times 108 M_{\odot}$ of primordial gas accreted at 13.0 Gyr.

^bAll the material expelled by Type II and Ia SNe during the last 2.5 Gyr is ejected to the IGM.

^cThe upper mass limit for the IMF amounts to $47 M_{\odot}$. Fraction of binary systems that become SNIa amounts to 0.02.

^dThe upper mass limit for the IMF amounts to $60 M_{\odot}$. Fraction of binary systems that become SNIa amounts to 0.02.

Model 8S in order to reproduce M_{gas} , O/H, and C/O.

One way to reduce the O/H and C/H values, maintaining the C/O ratio, is with a well mixed outflow of longer duration. In Model 8S, we assume a well mixed outflow during the first 4 Gyr of star formation and the m_{up} of IMF and the A_{bin} of Model 7L, the best of the L series models. Model 8S reproduces marginally all observational constraints with the exception of N/O (see Table 5 and Figure 12).

The C budget for Model 8S is practically the same than for Model 7L (see Table 4) because both models have the same SFR , IMF, A_{bin} and similar O/H.

During the wind phase the outflow rate of Model 8S is equal to 3.13 times the SFR . The gas mass lost is $7.2 \times 10^7 M_{\odot}$, 3.5 times the mass of stars formed during the first 4.0 Gyr of the star formation. Martin (1999) estimates outflow rates from 1.7 to 4.8 times the SFR for nearby irregular galaxies with the smallest maximum H I rotation speed of her sample. While these values are similar to those required by Model 8S, they are smaller than those required by Model 7L. The observed outflow rates for outbursting nearby irregular galaxies seem to support Model 8S over Model 7L, but probably at the time of the formation of the galaxy the accretion and merging of smaller structures also propitiated larger outflow rates, it is beyond the scope of this paper to carry this discussion further.

7.3. The N/O ratio

All our models fail to fit the N/O ratio, this could be due to problems with observations and with the adopted N yields. In what follows we will discuss this problem.

Carigi et al. (2005) obtained an excellent agreement between the present time N/O value predicted by the solar vicinity model and the N/O values derived from observations of H II regions of the solar vicinity. Alternatively, the N/O values predicted by all our models are higher than those observed in NGC 6822 by Peimbert et al. (2005).

Moreover the N/O values derived from metal poor stars are in agreement with the model by Carigi et al. (2005) but not for metal rich stars, these authors suggest that the disagreement is due

to the N yields adopted in the chemical evolution models.

We consider the M92 yields for C and O for Z_{\odot} as the best in the literature and we have used them in this paper. Unfortunately M92 did not compute the N yields. In this paper we have adopted the N yields for Z_{\odot} by MM02. The N yield is not self consistent with the C and O yields. Furthermore since the N abundance is considerably smaller than that of C and O, the predictions for these two elements are robust, but the N results for massive stars should be taken with caution.

Romano, Tosi, & Matteucci (2005) using N yields for LIMS by van der Hoek & Groenewegen (1997), different to those adopted by us, cannot reproduce the N/O values of NGC 1705, a late type dwarf galaxy. On the other hand, Gavilán, Mollá, & Buell (2005) using their own N yields are able to match the present-day N/O value of the solar vicinity, but not the N/O evolution. This problem should be studied further.

A possible explanation for the low N/O values in H II regions of NGC 6822 could be due to the escape of an important fraction of the ionizing photons. If such were the case, the ionization correction factor (ICF) for N becomes considerably larger than the usual ICF adopted (Peimbert et al. 2005; Relaño et al. 2002).

8. Discussion

The chemical evolution of NGC 6822 depends on M_{total} , the MAH, the baryonic infall as a function of time, and the importance of outflows. In what follows we will discuss these parameters and how they affect the different models that we have computed.

8.1. Total mass

From the cosmological model adopted we have found an $M_{total} = 2.6 \times 10^{10} M_{\odot}$. In what follows we will discuss possible upper and lower limits for M_{total} . In Figure 13 we present f_{acc} as a function of time for the minimum, adopted, and maximum M_{total} values.

The minimum M_{total} for the L models is obtained when there are no outflows present. For the mean MAH and without outflows we obtain $M_{total} = 1.54 \times 10^{10} M_{\odot}$, for a smaller mass the cosmological context predicts a smaller accreted

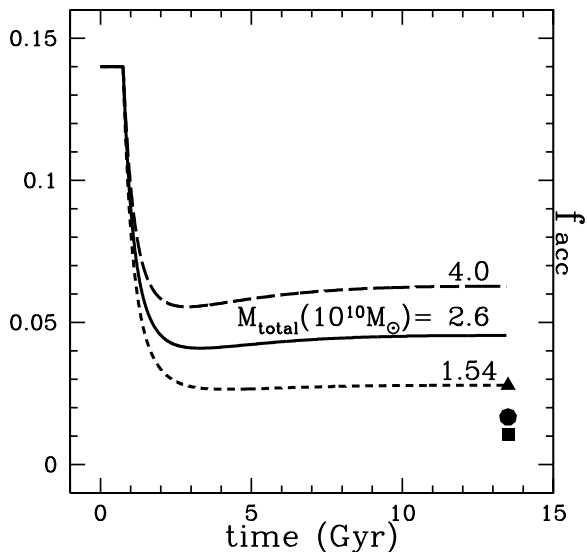


Fig. 13.— f_{acc} , the ratio of the baryonic mass accreted by galaxy to the total mass, as a function of time for the minimum, the adopted, and the high M_{total} values. The triangle, the circle and the square represent the ratio of the baryonic mass observed to the M_{total} for the $1.54 \times 10^{10} M_{\odot}$, $2.6 \times 10^{10} M_{\odot}$, and $4.0 \times 10^{10} M_{\odot}$, respectively.

mass than the baryonic mass observed. We have computed a chemical evolution model for this total mass and find that $12 + \log O/H = 8.66$ and $C/O = -0.29$ dex. The O/H value is considerably higher than the observed one. To fit the observed O/H value we need an O-rich outflow or to reduce m_{up} . In both cases the C/O value becomes considerably larger than observed. For example a model with m_{up} of $45 M_{\odot}$ gives $12 + \log O/H = 8.42$ in agreement with observations, but it also gives a $C/O = -0.13$ dex, 1.5σ higher than the observed value. Therefore the minimum M_{total} model can be discarded by the chemical evolution models. For the S models the minimum M_{total} is smaller than $2.6 \times 10^{10} M_{\odot}$ but larger than $1.54 \times 10^{10} M_{\odot}$.

The upper limit to M_{total} considered by us is $4 \times 10^{10} M_{\odot}$. The mass of this model is 1.54 times higher than the mass derived in section 3.2. For this model the accreted gaseous mass amounts to $25.1 \times 10^8 M_{\odot}$ and the ejected mass to $20.8 \times 10^8 M_{\odot}$. The ejected gaseous mass is about a fac-

tor of three larger than that of Model 7L and implies that the efficiency and the duration of the outflows have to be considerably larger than for Model 7L. If we assume a wind phase of 5.1 Gyr duration, like that of Model 7L, the outflow phase required amounts to 20.1 times the SFR . This value is about an order of magnitude larger than that derived by Martin (1999) for nearby irregular galaxies. The star formation history, that drives the outflow, is observationally fixed, and does not change with the increase of the adopted M_{total} . Moreover the larger M_{total} provides a larger gravitational field that reduces the possibility of extended outflows. From these arguments we consider the adopted upper limit for M_{total} a generous one.

Based on the models by van den Bosch (2003), that predict the virial masses of disk galaxies, we can also derive the masses for NGC 6822 for the cases with and without outflows. We have two observational constraints to derive M_{total} , the maximum rotational velocity, that amounts to 55 km s^{-1} , and the K luminosity that amounts to $\log(L_{tot}/L_{\odot}) = 8.5$. The $(L_{tot}/L_{\odot})_K$ ratio is obtained from the NGC 6822 and the solar M_K magnitudes that amount to -17.91 and 3.33 respectively (see Table 2, Campins et al. 1985, and Hayes 1985). From the two observational constraints and the models by van den Bosch with $Z = 0.007$ and no outflows we obtain $M_{total} \sim 1 \times 10^{10} M_{\odot}$, while for the models with $Z = 0.007$ and outflow we obtain $M_{total} = (2.0 \pm 0.5) \times 10^{10} M_{\odot}$; these values are somewhat smaller but in good agreement with those derived by us. Valenzuela et al. (2005) find $M_{total} 1.93 \times 10^{10} M_{\odot}$ and $3.4 \times 10^{10} M_{\odot}$ for their two favored models of NGC 6822 in good agreement with with our determination.

From the computed chemical evolution models we consider that the M_{total} adopted by us is reasonable. But if M_{total} were very different from our adopted value, new chemical evolution models must be computed.

8.2. Mass assembly history

In Figure 1 we have presented three MAHs, the slow, the mean, and the fast. In the models presented in this paper we have adopted the mean MAH. We will discuss why the other MAHs were not considered. In Figure 14 we show the f_{acc} for

the L models as a function of time for the three MAHs under discussion and under the assumption that $M_{total} = 2.6 \times 10^{10} M_{\odot}$. Due to the effects of reionization the amount of gas accreted by the galaxy reaches $8.5 \times 10^8 M_{\odot}$, $11.7 \times 10^8 M_{\odot}$, and $17.0 \times 10^8 M_{\odot}$ for the slow, the mean, and the fast MAHs respectively. The difference between the accreted mass and the observed baryonic mass, that amounts to $4.3 \times 10^8 M_{\odot}$, has to be ejected by outflows.

The infall of gas produced by the slow MAH at early times is not enough to form the older stars observed in NGC 6822. Therefore, based on our models, we discard the slow MAH.

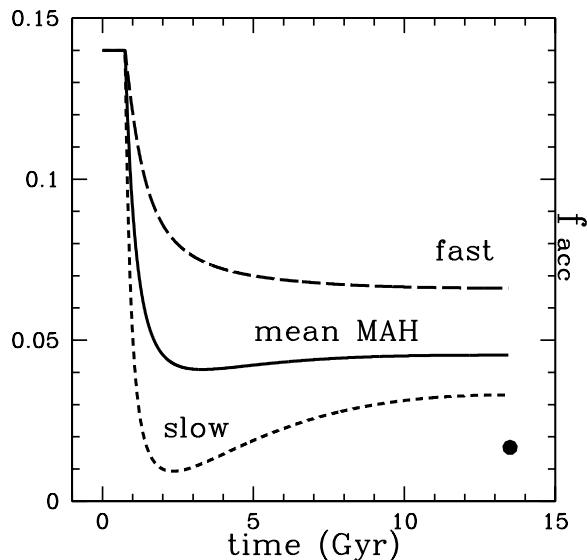


Fig. 14.— f_{acc} , the ratio of the baryonic mass accreted by the galaxy to the total mass, as a function of time for the slow, mean, and fast MAHs for $M_{total} = 2.6 \times 10^{10} M_{\odot}$. The filled circle is the ratio of the baryonic mass observed to the total mass for the three MAHs.

From Figures 1 and 14 it follows that we require to lose a larger amount of mass due to outflows for the fast than for the mean MAH models. Therefore the fast MAH models would require an early outflow of longer duration than the mean MAH models, typically of about 8 Gyr. Furthermore the gravitational field becomes larger at earlier times for the fast MAH than for the mean MAH models making it harder for outflows to occur, and the relative large initial gas content combined with the

observed star formation history also prevent the presence of large outflow rates. These considerations made us discard the fast MAH models.

8.3. Large and small infall models

As mentioned in section 3.4 several authors have suggested that a significant fraction of baryons is not accreted by the galaxies due to large-scale shock heating of the gas. To consider this possibility we have computed a series of S models assuming that the evolution up to $t = 5.37$ Gyr is the same as for the L models, but after this time accretion stops for the S models. The S models accrete only 60% of the mass accreted by the L models (see Figures 2 and 3).

The total mass accreted by the S models amounts to $7 \times 10^8 M_{\odot}$, and since the baryonic mass at present is $4.3 \times 10^8 M_{\odot}$, these models only require to lose $2.7 \times 10^8 M_{\odot}$. In Figure 15 we present f_{gal} , the ratio of the mass in baryons that remains in the galaxy to the total mass as a function of time.

In general the S models predict higher enrichments in O/H and C/H than the L models (see Tables 3 and 5). Model 8S, the best model of the S series, requires a well mixed outflow with a duration of 4.0 Gyr at the beginning of the *SFR*; its O/H, C/H, and M_{gas} values are 1.25σ , 1.4σ and 1σ higher than observed. Based on the chemical evolution models we favor the large-infall series over the small-infall one, particularly we prefer Model 7L over Model 8S.

If the effect of large-scale shock heating on gas accretion involves a fraction of baryonic matter smaller than that taken into account by the S series models, it will be possible to build successful galactic chemical evolution models, intermediate between Models 7L and 8S.

9. Conclusions

We have derived the *SFR* for NGC 6822 based on observations and photometric evolution models. Our photometric models based on the adopted *SFR*, the Salpeter IMF, the KTG IMFs, and three $Z(t)$ functions (those predicted by our best chemical evolution models, 7L and 8S, and that by Wyder) predict absolute magnitudes and colors that agree with the observed ones at the one σ level. This result implies that our derived *SFR* is

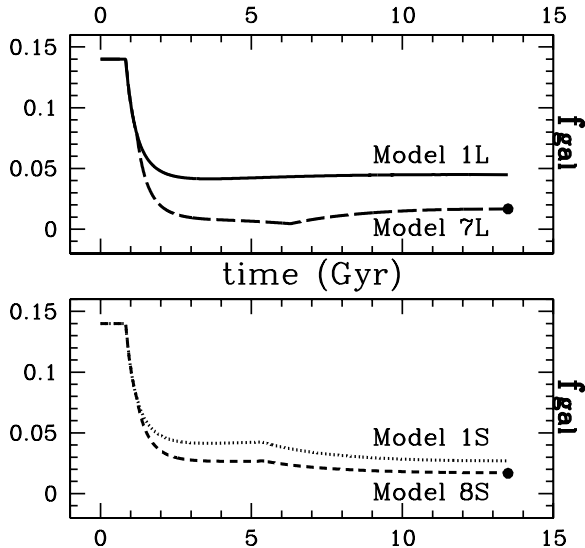


Fig. 15.— f_{gal} , the ratio of the mass in baryons that remains in the galaxy to the total mass, as a function of time. In the upper panel we show two large infall models: Model 1L, without outflows, and Model 7L our best model that includes an early outflow. In the lower panel we show two small infall models: Model 1S with no outflows and Model 8S that includes an early outflow. Note that for Models 1S and 1L $f_{gal} \equiv f_{acc}$. Filled circles represent the observational data.

robust and can be used for different applications related to NGC 6822.

Based on the adopted SFR we present 15 chemical evolution models for NGC 6822. All models evolve according to the mass assembly history of non baryonic mass predicted by a cosmological context. To distinguish among them we have used five additional observational constraints: M_{gas} , O/H, C/O, N/O, and Fe/O.

From the cosmological context adopted and our chemical and photometric evolution models for NGC 6822 we find that $1.54 < M_{total}(10^{10}M_{\odot}) < 4.0$. The adopted mass for the 15 models presented in Tables 3 and 5 is $2.6 \times 10^{10} M_{\odot}$. Based on similar arguments, of the three MAHs considered, we adopt the mean MAH for all our models.

For the models of the large infall series, we have assumed that during accretion the universal baryon fraction is only reduced by reioniza-

tion. For the models of the small infall series, we have assumed that accretion of baryonic matter is further reduced by large-scale gas shock heating. The best models of each series, Models 7L and 8S, produce a reasonable fit to the observational constraints, but Model 7L is somewhat better.

Models without well mixed outflows are not successful in reproducing the observational constraints because the amount of baryonic gas accreted by the galaxy is higher than the amount of baryonic matter derived from observations. Moreover based on our adopted SFR the thermal heating produced by SNe, under the assumption of no outflows, is considerably larger than the binding energy of the observed gas content. These two results imply that the presence of outflows of well mixed material is needed. We argue that these outflows most likely occurred early on in the history of the galaxy.

In order to comply with the presence of an early outflow, and the observed O/H and C/H values, we have computed our best models (Model 7L and 8S) that have a KTG IMF with m_{up} of $60 M_{\odot}$ while for the solar vicinity m_{up} amounts to $80 M_{\odot}$. That is the number of SN of Type II per generation of stars has to be smaller in NGC 6822 than in the solar vicinity. A lower value of m_{up} for NGC 6822 than for the solar vicinity is in agreement with recent results on dwarf galaxies by others authors.

According to Models 7L and 8S and the observed Fe/O value the fraction of binary systems that become SNIa in NGC 6822 is 2 % while in the solar vicinity amounts to 5 %.

The fractions of C produced by MS ($m > 8M_{\odot}$), LIMS ($m < 8M_{\odot}$), and SNIa amount to 60 – 63%, 38 – 36%, and 1 – 2% respectively. On the other hand, in the solar vicinity, these values amount to 48%, 50%, and 2%, respectively.

The N/O values predicted by all our models are higher than observed, the discrepancy could be due to the N ionization correction factor adopted to derive the N abundance in H II regions and to the N stellar yields adopted by our chemical evolution models.

The results obtained in this paper apply to an isolated typical irregular galaxy, but do not apply to irregular galaxies that have suffered strong tidal effects.

Further progress in modelling NGC 6822 can

come if a more precise M_{total} is determined, and if the issue about the large-scale gas shock heating is finally settled.

L.C. thanks Gustavo Bruzual for instructing her how to use the GALAXEV code including a metal enrichment history, and for computing a set of photometric properties for instantaneous-burst models based the KTG IMF. L.C. is also grateful to Ted K. Wyder for several illuminating explanations about the star formation history of NGC 6822. P.C. thanks A. Kravtsov for kindly providing information about mass assembly histories in simulations. We acknowledge Octavio Valenzuela for valuable conversations and thank Vladimir Avila-Reese for helpful suggestions. We are grateful to Donatella Romano for a critical reading of the manuscript. We also acknowledge to the anonymous referee for a careful reading of the manuscript and many excellent suggestions. LC's work is supported by CONACyT grant 36904-E. PC acknowledges support by CONACyT grant 36584-E. MP received partial support from DGAPA UNAM (grant IN114601).

REFERENCES

- Akerman, C. J., Carigi, L., Nissen, P. E., Pettini, M., & Asplund, M. 2004, *A&A*, 414, 931
- Allende Prieto, C., Barklem, P. S., Lambert, D. L., & Cunha, K. 2004, *A&A*, 420, 183
- Arnouts et al. 2005, *ApJ*, 619, L43
- Asplund, M., Grevesse, N., & Sauval, A. J. 2005, in: *Cosmic Abundances as Records of Stellar Evolution and Nucleosynthesis*, ed. F. N. Bash & T. G. Barnes, ASP Conference Series, 336, 25
- Avila-Reese, V., Firmani, C., & Hernández, X. 1998, *ApJ*, 505, 37
- Bond, J.R., Cole, S., Efstathiou, G., & Kaiser, N. 1991, *ApJ*, 379, 440
- Bower, R. 1991, *MNRAS*, 248, 332
- Bullock, J.S., Kolatt, T.S., Sigad, Y., Somerville, R.S., Kravtsov A.V., Klypin, A.A., Primack, J.R., & Dekel, A. 2001, *MNRAS*, 321, 559
- Bruzual, G., & Charlot, S. 2003, *MNRAS*, 344, 1000
- Campins, H., Rieke, G. H., & Lebofsky, M. J. 1985, *AJ*, 90, 896.
- Carigi, L. 2003, *MNRAS*, 339, 825
- Carigi, L., Colín, P., & Peimbert, M. 1999, *ApJ*, 514, 787
- Carigi, L., Colín, P., Peimbert, M., & Sarmiento, A. 1995, *ApJ*, 445, 98.
- Carigi, L., Hernández, X., & Gilmore, G. 2002 *MNRAS*334, 117
- Carigi, L., Peimbert, M., Esteban, C., & García-Rojas, J. 2005, *ApJ*, 623, 213
- Chieffi, A., & Limongi, M. 2002 *ApJ*, 577, 281
- Christensen-Dalsgaard, J. 1998, *Space Sci. Rev.*, 85, 19
- Cowie, L.L., Songaila, A., Hu, E.M., & Cohen, J.G. 1996, *ApJ*, 112, 839
- Coxi, D.P., 1972, *ApJ*, 178, 159
- Cunha, K., & Lambert, D. L. 1994, *ApJ*, 426, 170
- Davé, R., Cen, R., Ostriker, J.P., Bryan, G., Hernquist, L., Katz, N., Weinberg, D.H., Norman, M.L., & O'Shea, B. 2001, *ApJ*, 552, 473
- De Blok, W. J. G. & Walter, F. 2006 *AJ*, 131, 343
- Esteban, C., Peimbert, M., García-Rojas, J., Ruiz, M.T., Peimbert, A., & Rodríguez, M. 2004, *MNRAS*, 355, 229
- Fragile, P. C., Murray, S. D., & Lin, D. N. C. 2004, *ApJ*, 617, 1077
- Fujita, A., Mac Low, M. M., Ferrara, A., & Meiksin, A. 2004, *ApJ*, 613, 159
- Fukugita, M., & Peebles, P.J.E. 2004, *ApJ*, 616, 643
- Garnett, D. R. 2002, *ApJ*, 581, 1019
- Gavilán, M., Mollá, M. & Buell, J. F. 2005, *A&A*, submitted (astro-ph/0601326)
- Gnedin, N.Y. 2000, *ApJ*, 542, 535

- Goodwin, S. P., & Pagel, B. E. J. 2005, *MNRAS*, 359, 707
- Gottesman, S. T., & Welichew, L. 1977, *Å*, 61, 523
- Hayes, D. S. 1985, in “Calibration of fundamental stellar quantities”, IAU Symp. 111, ed. D. S. Hayes et al. (Reidel: Dordrecht), 225
- Hodge, P. W. 1977, *ApJS*, 33, 69
- Huchtmeier, W. K., & Richter, O.-G. 1986 *A&AS*, 63, 323
- Israel, F.P. 1997, *A&A*, 317, 65
- Jarrett, T. H., Chester, T., Cutri, R., Schneider, S. E., & Huchra, J. P. 2003, *AJ*, 125, 525
- Kang, H., Ryu, D., Cen, R., & Song, D. 2005, *ApJ*, 620, 21
- Kravtsov, A.V., Gnedin, O.Y., & Klypin, A.A. 2004, *ApJ*, 609, 42
- Kroupa P., Tout C.A., Gilmore G. 1993, *MNRAS*, 262, 545 (KTG)
- Lacey, C., & Cole, S. 1993, *MNRAS*, 262, 627
- Lanfranchi, G.A., & Matteucci, F. 2003, *MNRAS*, 345, 71
- Larsen, T.I., Sommer-Larsen, J., & Pagel, B.E.J. 2001, *MNRAS*, 323, 555
- Lee, H., Skillman, E.D., & Venn, K.A. 2006, *ApJ*, accepted (astro-ph/0512428)
- Legrand, F., Tenorio-Tagle, G., Silich, S., Kunth, D., & Cerviño, M. 2001, *ApJ*, 560, 630
- Maeder, A. 1992, *A&A*, 264, 105
- Maller, A.H., Katz, N., Kereš, Dave, R., & Weinberg, D. 2005, *MNRAS*, submitted (astro-ph/0509474).
- Marigo, P., Bressan, A., & Chiosi, C. 1996, *A&A*, 313, 545
- Marigo, P., Bressan, A., & Chiosi, C. 1998, *A&A*, 331, 564
- Martin, C. 1999, *ApJ*, 513, 156
- Martin, C. 2003, *Rev. Mexicana Astron. Astrofís. Ser. Conf.*, 17, 56
- Meynet, G., & Maeder, A. 2002, *A&A*, 390, 561
- Mo, H.J., Yang, X., van den Bosch, F.C., & Katz, N. 2005, *MNRAS*, 363, 1155
- Muschielok, B. et al. 1999, *A&A*, 352, L40
- Navarro, J.F., Frenk, C.S., & White, S.D.M. 1995, *MNRAS*, 275, 720
- Navarro, J.F., Frenk, C.S., & White, S.D.M. 1996, *ApJ*, 462, 563
- Navarro, J.F., Frenk, C.S., & White, S.D.M. 1997, *ApJ*, 490, 493
- Pagel, B. E. J., Edmunds, M. G., Fosbury, R. A. E., & Webster, B. L. 1978, *MNRAS*, 184, 569
- Peimbert, A., Peimbert, M., & Ruiz, M. T. 2005, *ApJ*, 634, 1056
- Portinari, L., Chiosi, C., & Bressan, A. 1998, *A&A*, 334, 505
- Relaño, M., Peimbert, M., & Beckman, J. 2002, *ApJ*, 564, 704
- Romano, D., Tosi, M., & Matteucci, F. 2005, *MNRAS*, 365, 759
- Salpeter, E. E. 1955 *ApJ*121, 161
- Sawa, T., & Fujimoto, M. 2005, *PubASJ*, 57, 429
- Schlegel et al. 1998, *ApJ*, 500, 525
- Tenorio-Tagle, G., Silich, S., & Muñoz-Tuñón, C., 2003, *Rev. Mexicana Astron. Astrofís. Ser. Conf.*, 18, 136
- Thielemann, F. K., Nomoto, K., & Hashimoto M. 1993, in “Origin and Evolution of the Elements” eds. N. Prantzos et al., Cambridge University Press, p. 297
- Trimble, V. 2000, in *Allen’s Astrophysical Quantities*, ed. A. N. Cox, (Springer-Verlag: New York), 578
- Valenzuela, O., Rhee, G., Klypin, A., Stinson, G., Governato, F., Quinn, T. & Wadsley, J. 2005, *ApJ*, submitted (astro-ph/0509644)

- van den Bosch, F. 2002, MNRAS, 331, 98
- van den Bosch, F. 2003, in “The Mass of Galaxies at High and Low Redshift”, ESO, 250, (astro-ph/0201006)
- van der Hoek, L. B., & Groenewegen, M. A. T. 1997, A&AS, 123, 305
- Veilleux, S., Cecil, G., & Bland-Hawthorn, J. 2005, ARA&A, 43, 769
- Venn, K. A., Lennon, D. J., Kaufer, A., McCarthy, J. K., Przybilla, N., Kudritzki, R. P., Lemke, M., Skillman, E. D., & Smartt, S. J. 2001, ApJ, 547, 765
- Venn, K. A., & Miller, L. 2002, Rev. Mexicana Astron. Astrofís. Ser. Conf., 12, 230
- Weldrake, D. T. F., de Block, W. J. G., & Walter, F. 2003, MNRAS, 340, 12
- Weidner, C., & Kroupa, P. 2005, ApJ, 625, 754
- Wyder, T. K. 2001, AJ, 122, 2490
- Wyder, T. K. 2003, AJ, 125, 3097